

Human-like Energy Management Based on Deep Reinforcement Learning and Historical Driving Experiences

Teng Liu, Xiaolin Tang, Xiaosong Hu, *Senior Member, IEEE*, Wenhao Tan, Jinwei Zhang

Abstract—Development of hybrid electric vehicles depends on an advanced and efficient energy management strategy (EMS). With online and real-time requirements in mind, this article presents a human-like energy management framework for hybrid electric vehicles according to deep reinforcement learning methods and collected historical driving data. The hybrid powertrain studied has a series-parallel topology, and its control-oriented modeling is founded first. Then, the distinctive deep reinforcement learning (DRL) algorithm, named deep deterministic policy gradient (DDPG), is introduced. To enhance the derived power split controls in the DRL framework, the global optimal control trajectories obtained from dynamic programming (DP) are regarded as expert knowledge to train the DDPG model. This operation guarantees the optimality of the proposed control architecture. Moreover, the collected historical driving data based on experienced drivers are employed to replace the DP-based controls, and thus construct the human-like EMSs. Finally, different categories of experiments are executed to estimate the optimality and adaptability of the proposed human-like EMS. Improvements in fuel economy and convergence rate indicate the effectiveness of the constructed control structure.

Index Terms—Hybrid electric vehicles, deep reinforcement learning, human-like, energy management strategy, dynamic programming

NOMENCLATURE

HEV	Hybrid Electric Vehicles
PHEV	Plug-in Hybrid Electric Vehicle
EMS	Energy Management Strategy
RL	Reinforcement Learning
DRL	Deep Reinforcement Learning
DQL	Deep Q-learning
DDPG	Deep Deterministic Policy Gradient
NN	Neural Network
DP	Dynamic Programming
ICE	Internal-Combustion Engine

ISG	Integrated Starter Generator
SoC	State of Charge
BSFC	Brake Specific Fuel Consumption
GPS	Global Position System
MDP	Markov Decision Process

I. INTRODUCTION

HAVING potentials in energy conservation and pollution reduction, the hybrid electric vehicles (HEVs) and plug-in hybrid electric vehicles (PHEVs) are becoming mass-market electrified vehicles in the current sales market [1-5]. Energy management and powertrain matching are two crucial technologies to improve fuel economy and maintain excellent performance for these vehicles [6, 7]. How to operate these vehicles in an ideal pattern for power distribution is an arduous task called energy management strategies (EMSs) [8-10].

Sophisticated multiple energy storage resources in hybrid powertrain require advanced EMS to achieve power cooperation in different driving situations [11, 12]. Three categories of EMSs are presented to resolve the energy management (power split) problems for different powertrain architectures until now, which are the rule-, optimization- and learning-based policies [13-15]. How to implement these excellent EMSs into real-world driving environments to construct human-like power split controls is still a research priority in the current energy management field.

Motivated by the remarkable development of deep learning and reinforcement learning (RL) in artificial intelligence, deep reinforcement learning (DRL) is regarded as a promising methodology to derive intelligent EMS for hybrid powertrain [16, 17]. For example, the authors in [18] applied well-known deep Q-learning (DQL) to address the continuous optimization control problem in energy management and achieve impressive performance. To improve the convergence rate, Qi et al. [19] used dueling DQN to solve the energy management problem for a parallel powertrain, and the proposed control policy is proven to be better than onboard binary control. Furthermore, Ref. [20] and [21] utilized a deep deterministic policy gradient (DDPG) to derive the optimal EMS for Prius and series-parallel PHEV, respectively. The induced DDPG-enabled control policy is compared with the conventional DRL methods and is certified to have a better fuel economy. However, since multiple neural networks (NN) exist in these DRL approaches, it is a time-consuming process to obtain mutable DRL-based EMS. Hence, these derived control policies are not able to be applied in real-world driving environments.

This work was in part supported by the State Key Laboratory of Mechanical System and Vibration (Grant No. MSV202016), National Natural Science Foundation of China (Grant No. 51875054), and Chongqing Natural Science Foundation for Distinguished Young Scholars (Grant No. cstc2019jcyj0010), Chongqing Science and Technology Bureau, China. (Corresponding authors: X. Tang and X. Hu.)

T. Liu, X. Tang, X. Hu, and W. Tan are with Department of Automotive Engineering, Chongqing University, Chongqing 400044, China (email: tengliu17@gmail.com, tangxl0923@cqu.edu.cn, xiaosonghu@ieee.org, 201932131033@cqu.edu.cn).

J. Zhang is with Department of Mechanical and Mechatronics Engineering, University of Waterloo, N2L 3G1, Canada. (jinwei.zhang@uwaterloo.ca)

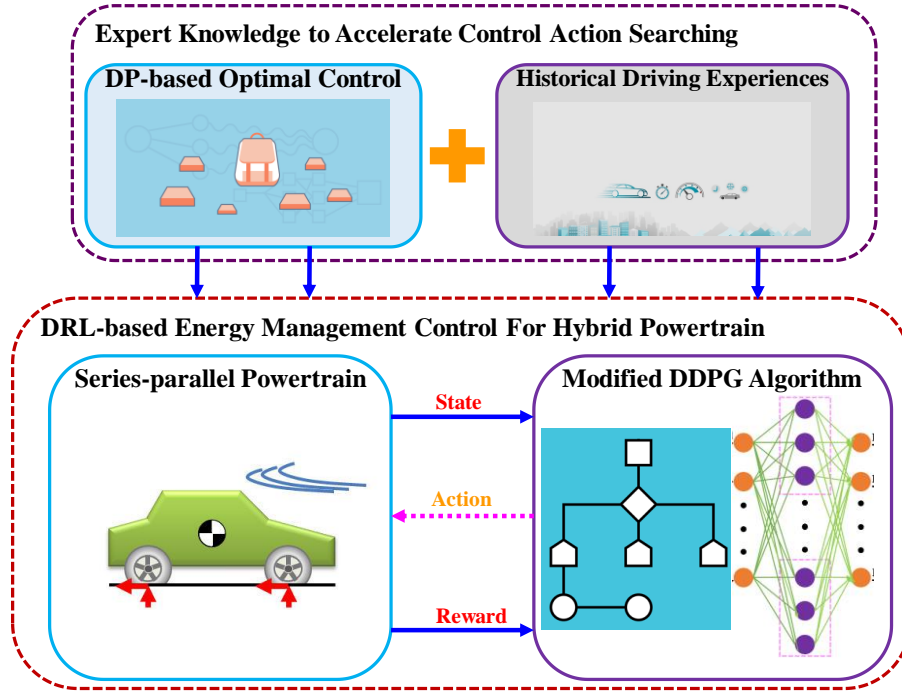


Fig. 1. Human-like energy management system with expert knowledge for HEV.

In this article, a human-like energy management framework is constructed depending on the DRL technique and collected historical driving data, as depicted in Fig. 1. First, a series-parallel hybrid powertrain is modeled and treated as the testified target of the presented EMS. Then, the modified DDPG-enabled control construction is introduced, wherein the dynamic programming (DP)-based optimal global control or collected historical driving data from experienced drivers are considered as expert knowledge to enhance the searching space for control actions. By doing this, a human-like driving policy is generated and its optimality and convergence rate are guaranteed. Finally, the standard and real-world driving cycles are employed to evaluate the optimality and adaptability of the proposed human-like EMS.

Three perspectives of contributions and innovations are included in this paper: 1) a human-like EMS is presented based on the DRL approach and collected historical driving data; 2) a modified DDPG framework is founded, and it is embedded with DP-enabled optimal control actions; 3) Guided by the real-world driving behaviors, the proposed human-like control policy is able to adapt to different driving cycles. This paper is one attempt to combine the DRL method and real-world driving data, which is one possible solution for online or real-time power split controls for HEVs/PHEVs.

The following construction of this paper is arranged as follows: the series-parallel hybrid powertrain and its relevant energy management problem is given in Section II. The improved DDPG technique, DP method, and collected real-world driving data are introduced in Section III. Section IV describes the simulation results to estimate the proposed control structure, and its relevant optimality and adaptability are analyzed and certified. Finally, the conclusion and future work are summarized in Section V.

II. POWERTRAIN MODELING AND ENERGY MANAGEMENT PROBLEM

The studied hybrid powertrain has a series-parallel topology, and its control architecture is shown in Fig. 2 [22]. The primary components are the internal-combustion engine (ICE), lithium-ion battery pack, traction motor, and integrated starter generator (ISG). The energy management controller is capable of distributing the output power between ICE and battery in order to realize the optimization control objectives. The following content elucidates the mathematical completeness of this powertrain modeling. The values of the main parameters are exhibited in Table I.

A. Powertrain Modeling

As the driving cycle is given in advance, the vehicle speed and acceleration are determined. Thus, the power demand P_d of the whole powertrain is represented by three parts as follow:

$$P_d = P_r + P_a + P_i \quad (1)$$

$$P_r = f \cdot M_v \cdot g \cdot v \quad (2)$$

$$P_a = \frac{1}{2} \rho A_a C_D v^2 \cdot v \quad (3)$$

$$P_i = M_v a \cdot v \quad (4)$$

where P_r , P_a , and P_i are the powers related to the rolling resistance, aerodynamic drag, and inertial force, respectively. M_v is the curb weight, g is the gravity coefficient, ρ is the air density, A_a is the frontal area, f and C_D are the coefficients of rolling resistance and aerodynamic drag, respectively. v and a are the vehicle speed and acceleration and they are mutable in different driving cycles, and hence the power demand changes with the

driving cycle. It implies that the energy management controller should adjust its EMS to adapt to different driving conditions.

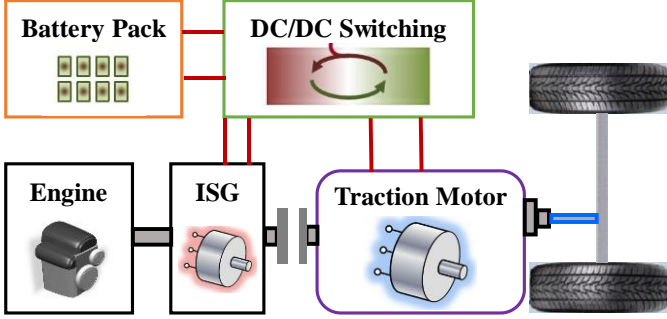


Fig. 2. Configuration of studied series-parallel powertrain topology [22].

The power request is supplied by two onboard energy storage systems, battery, and ICE. In the battery, the state of charge (SoC) indicates the remaining electric capacity after running the specific driving cycle. The value of SoC ranges from 0 to 1 and its variation can be computed by:

$$\dot{SoC} = -I_b / Q_c \quad (5)$$

where Q_c and I_b are the nominal capacity and output current of the battery, respectively. To simulate the battery as internal resistance model [23], the output power P_b and voltage U_b of battery are written as follow:

$$P_b = U_b \cdot I_b \quad (6)$$

$$U_b = V_{oc} - I_b r_0 \quad (7)$$

where V_{oc} is the open-circuit voltage, and r_0 implies the internal resistance. Incorporating the Eq. (5) to (7), the variation of SoC is able to be described as:

$$\dot{SoC} = -(V_{oc} - \sqrt{V_{oc}^2 - 4r_0 P_b}) / (2Q_c r_0) \quad (8)$$

To maintain the long service life of the battery, it should not be overcharged or over-discharged. Hence, the value of SoC is assumed to belong to [0.2, 0.9] in this work. For this series-parallel powertrain, the nominal capacity of the battery is 8.1Ah, with the nominal voltage of 200V and internal resistance of 0.25Ω. Since the output power of the battery is decided by power demand and power of ICE, the SoC can be calculated by Eq. (8) at arbitrary time instant. Therefore, SoC is chosen as one state variable to suggest the performance of control actions.

TABLE I [22]
POWERTRAIN PARAMETERS FOR THE STUDIED SERIES-PARALLEL HEV

Symbol	Implication	Values
M_v	Curb weight	1325 kg
ρ	Air density	1.225 kg/m ³
f	Rolling resistance coefficient	0.012
A_a	Frontal area	2.16 m ²
C_D	Aerodynamic drag coefficient	0.26
g	Gravity coefficient	9.8 m/s ²
V_{oc}	Open circuit voltage	150 V
SoC_{ref}	Charge sustaining value	0.6

The significant parameter in ICE is the fuel consumption rate,

which reflects the fuel economy of HEV directly. Modeled by static map method, the fuel consumption rate m_f is determined by the speed and torque of ICE as follow:

$$m_f = f_e(T_e, \omega_e) \quad (9)$$

where T_e and ω_e are the torque and speed of ICE, respectively. f_e is always represented by the look-up table function, which means the brake specific fuel consumption (BSFC) curve of ICE is mutable in this work.

The speed range of ICE in this series-parallel powertrain is 1000 rpm to 4500 rpm, the peak power is 57 kW at 5000 rpm, and peak torque is 115 Nm at 4200 rpm. Assuming power demand is known a priori, the output power of ICE can decide battery power and SoC, and thus the ICE power is selected as control actions in this article with continuous space [22].

B. Energy Management Formulation

The energy management problem of HEV is converted into an optimization control problem with a predefined objective and several constraints. The goal of this problem is to search a control sequence to achieve the best control performance. The control objective is usually represented by the cost function J over a finite time horizon as follow:

$$\begin{cases} J = \int_0^T [m_f(t) + \delta(\Delta_{SoC}(t))^2] dt \\ \Delta_{SoC}(t) = \begin{cases} SoC(t) - SoC_{ref} & SoC(t) < SoC_{ref} \\ 0 & SoC(t) \geq SoC_{ref} \end{cases} \end{cases} \quad (10)$$

wherein the first term is the fuel economy and the second one means the charge sustaining restraint. δ is a positive weighting parameter to tune these two goals in the cost function and it equals 500 in this work. SoC_{ref} is a pre-defined factor to guarantee the final value of SoC close to its initial value, and it is settled as 0.7 in this paper.

Generally, the cost function is affected by the state variable $s \in S$ and $a \in A$. In this paper, the state variables are the vehicle speed, acceleration and SoC, and the control action is the power of ICE:

$$S = \{v, a, SoC \in [0.2, 0.9]\} \quad (11)$$

$$A = \{P_e \in [0, 57]\} \quad (12)$$

To choose the best control actions from a normal working area, the defined optimization control problem should follow a couple of constraints. It implies that the ICE, battery, ISG, and traction motor need work in a reasonable range as:

$$\begin{cases} SoC_{min} \leq SoC(t) \leq SoC_{max} \\ P_{b,min} \leq P_b(t) \leq P_{b,max} \end{cases} \quad (13)$$

$$\begin{cases} \omega_{x,min} \leq \omega_x(t) \leq \omega_{x,max}, & x = m, g, e \\ T_{x,min} \leq T_x(t) \leq T_{x,max}, & x = m, g, e \end{cases} \quad (14)$$

where the symbol max and min denote the maximum and minimum value of the relevant variables. The subscript g and e indicate the torque and speed related to the generator and motor, respectively. In this work, the road scope of the driving cycle and influence of temperature for battery characteristics are not

considered. In the next section, the DDPG algorithm is introduced to derive the human-like EMS with expert knowledge. lower and upper bounds of the variables.

III. DRL ALGORITHM AND EXPERT KNOWLEDGE

This section aims to construct the DRL framework for the energy management problem of the series-parallel powertrain, wherein the particular DDPG algorithm is illuminated. To enhance the DDPG algorithm, the optimal control strategy obtained from DP is taken as expert knowledge to narrow the searching space of control actions. Furthermore, the collected process of a real-world driving dataset from experienced drivers is described. For an individual driving cycle, the appropriate collected ICE behaviors are also treated as expert knowledge to train the human-like energy management policy.

A. Dynamic Programming Method

According to Bellman's principle of optimality, DP enables to acquire the optimal global controls in a multi-step horizon optimization control problem by an exhaustive search of state variables and control actions [24]. Many attempts have executed to apply DP to address the HEV's energy management problems [25-27]. However, limited by the curse of dimensionality, DP cannot solve the problem with a large search space. Hence, the DP-based control strategy is often regarded as a benchmark to evaluate other EMSs.

Bellman's principle of optimality indicates that for a N -steps optimization control problem, if $a(m)$ ($m = 1, 2, \dots, N$) is the optimal control sequence over the whole time interval, then the truncated sequence $a(n)$ ($n = k+1, k+2, \dots, N$) is still the optimal control sequence for time horizon from $k+1$ to N . For example, the cost function in Eq. (10) can be rewritten as follow:

$$J_N = \varphi(s_N) + \sum_{k=1}^{N-1} L(s_k, a_k, k) \quad (15)$$

where φ is a restrictive function on the final value of state variables (SoC), and L is named instantaneous cost function, which is the sum of fuel consumption rate and charge sustaining restraint. Then, the optimal cost function J^* is minimizing or maximizing the cost function in Eq. (15) as:

$$J_N^* = \min \left\{ \varphi(s_N) + \sum_{k=1}^{N-1} L(s_k, a_k, k) \right\} \quad (16)$$

To search the optimal control at each time step, the Eq. (16) can be further formulated as the recursive expression as:

$$J_{N-k}^* = \min \{ J_{N-(k+1)}^* + L(s_k, a_k, k) \} \quad (17)$$

Executing Eq. (17) through a backward iteration process, the optimal control policy $[a^*_1, a^*_2, \dots, a^*_N]$ is able to be computed. Then the related state variable $[s^*_1, s^*_2, \dots, s^*_N]$ can be calculated by a recursive forward process.

In this work, as the DP algorithm could achieve the optimal control policy for an exceptional driving cycle, it can be imported into the DRL framework to be the expert knowledge. It implies that the relevant DRL algorithm would not search the optimal controls from the original space, as alternatives, it would gain the controls from the DP-based control policy. By doing this, the search space is narrowed, which would improve the computational time and convergence rate.

B. Historical Driving Experiences

In real-world driving environments, the experienced drivers could manage the driving strategy (indicates power split controls in this article) depend on the driving situations. For example, the drivers would make braking decisions beforehand when they cannot drive through the traffic lights at intersections. Moreover, they may make the ICE work in the area of high efficiency regularly to promote the fuel economy on the highway.

Inspired by these experienced and mature driving policies for HEVs, a series of experiments are designed to collect the historical driving dataset in HEVs. The experiments are implemented on several kinds of HEVs in Beijing, China [28]. The collected data includes vehicle velocity, acceleration, travel distance, global position system (GPS) data of the vehicle, the output power of ICE and battery, torque, and speed of motor and generator. The mentioned collected data is related to the daily life of each HEV, such as morning peak and evening peak. Hence, the obtained data could contain the driving cycles in highway and urban driving environments.

Fig. 3 depicts the terminal device and its configuration for data collection. The parameters of the hybrid powertrain are recorded from the distributed CAN bus, and the geographical information is stored by the GPS module. The collected data can be transferred into a cloud corner each day and stored as the Excel file. The sampling frequency of this data is 10Hz, which means its precision is enough for energy management research. Finally, the collection process lasts for 1320 days, 3885 times, and 45384 km. A part of them is selected and preprocessed for energy management research.

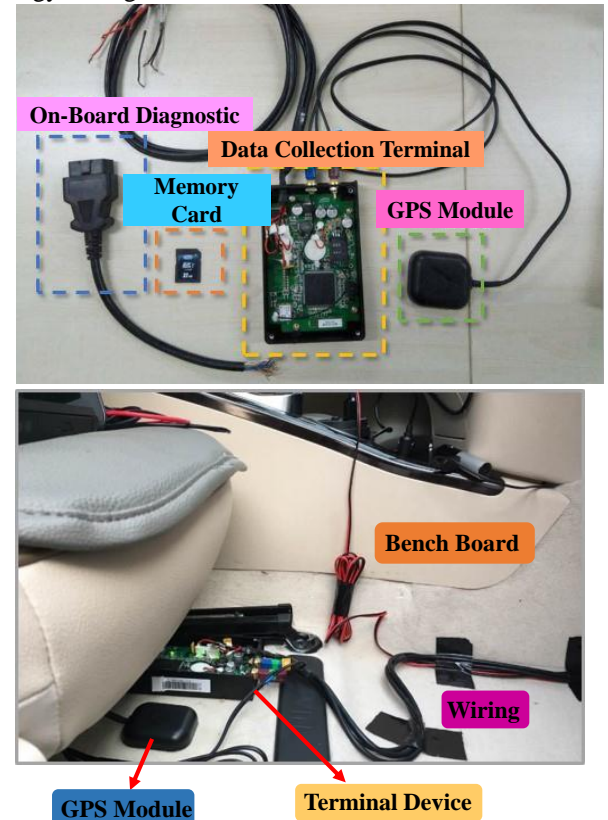


Fig. 3. Terminal device for historical driving data collection [5].

TABLE II [32]

Computational procedure of the modified DDPG algorithm with expert knowledge

Modified DDPG algorithm

1. Initialize critic network θ^Q and actor network θ^π , memory pool K , give initial values for α, β , number of episodes M and ε
2. Input DP-based control policy or real-world collected driving strategy (taken as expert knowledge)
3. for the episode in the range $[1, M]$ do
4. Give initial values for three states v_1, a_1, SoC_1
5. for t in the range $[0, T]$ do
6. Choose action $a_t = \pi(s_t | \theta^\pi)$ according to the expert knowledge (input optimal policy) and exploration noise
7. Receive r_t and s_{t+1} based on current action a_t and state s_t
8. Store transition model (s_t, a_t, r_t, s_{t+1}) in K
9. Sample a minibatch of transitions (s_t, a_t, r_t, s_{t+1}) from K with priority experience replay
10. Set $y_t = r(s_t, a_t) + \beta Q(s_{t+1}, a_{t+1} | \theta^Q)$
11. Update the critic by minimizing the loss function: $\nabla l(\theta^Q) = E[(r + \beta Q(s_{t+1}, a_{t+1} | \theta^Q) - Q(s_t, a_t | \theta^Q)) \nabla Q(s_t, a_t | \theta^Q)]$
12. Update the actor policy using the sampled policy gradient: $\nabla_{\theta^\pi} L \approx E[\nabla_{\theta^\pi} Q(s_{t+1}, a_{t+1} | \theta^Q)] = E[\nabla_a Q(s_t, a_t | \theta^Q) \nabla_{\theta^\pi} \pi(s_t | \theta^\pi)]$
13. Store the critic and actor network for experience replay
14. end for loop
15. end for loop

In [28], the fundamental properties of the collected driving experiences are compared and analyzed, such as acceleration interval distribution, velocity interval distribution, traction states and so on. The relevant results indicate the characteristics between standard and real-world driving cycles are extremely different. Thus, this paper would choose several real-world driving cycles to derive human-like EMS. It means the driving policy (especially the power split controls between battery and ICE) would be the guidance for controls search in the DRL framework. By doing this, the search space of control actions is narrowed too, and the optimal control actions would only select from the collected control in a real-world environment.

C. Modified DDPG Algorithm

Unlike other machine learning methods, RL discusses how to choose the best control actions based on the interaction between an agent and its environment [29]. Its supreme advantage is realizing self-improvement through a learning process, which is usually a trial-and-error search. It represents that the RL agent will try the control actions and evaluate them by the relevant rewards. It is essential that each action in RL affects not only the immediate but also the subsequent rewards.

Markov decision processes (MDPs) are a typical formalization of sequential decision making, in which the actions influence the immediate and subsequent rewards and states [30]. Hence, MDP is an ideal mathematical formulation of RL, and the interaction between the agent and environment is expressed as a $\langle \mathcal{S}, \mathbf{A}, \mathbf{P}, \mathbf{R}, \beta \rangle$. The \mathcal{S} and \mathbf{A} are the set of state variables and control actions given in Eq. (11) and (12). $p \in \mathbf{P}$ represents the transition model of the state in the environment, and $r \in \mathbf{R}$ is the reward model to estimate the selection of action. Finally, β is a discount factor to balance the significance of immediate and subsequent rewards.

The objective of the RL algorithm is to determine a control policy π to maximum the cumulated rewards. In general, the RL

algorithms are cast into policy-based (policy gradients algorithm) and value-based ones (Q-learning and Sarsa algorithms) [29]. Two value functions are defined to represent the cumulated rewards in value-based algorithms as follow:

$$V^\pi(s_t) = E\left(\sum_{t=0}^T \beta^t r(s_t, a_t)\right) \quad (18)$$

$$Q^\pi(s_t, a_t) = r(s_t, a_t) + \beta \sum_{s_{t+1} \in \mathcal{S}} p(s_{t+1} | s_t, a_t) Q(s_{t+1}, a_{t+1}) \quad (19)$$

where V^π and Q^π are the value functions followed by the control policy π , and $p(s_{t+1} | s_t, a_t)$ is the transition dynamic from s_t to s_{t+1} . Then, the standard Q-learning algorithm is settled to update the action-value function $Q(s, a)$ for control action selection:

$$Q(s_t, a_t) \leftarrow Q(s_t, a_t) + \alpha [r + \beta \max_{a_{t+1}} Q(s_{t+1}, a_{t+1}) - Q(s_t, a_t)] \quad (20)$$

where α is the learning rate. In each time step, the ε -greedy policy is applied to choose the control action. It implies that the agent would exploit the best action until now with probability $1-\varepsilon$, and explore the environment with probability ε . However, it is difficult for Q-learning to handle the continuous action spaces because the search space is too ample for greedy policy. Instead, DQL [31] is proposed to function approximately the action-value function Q with a neural network (NN), wherein the loss function is described as:

$$l(\theta^Q) = E[(Q(s_t, a_t | \theta^Q) - y_t)^2] \quad (21)$$

$$y_t = r(s_t, a_t) + \beta Q(s_{t+1}, a_{t+1} | \theta^Q)$$

where $l(\theta^Q)$ is the loss function and θ^Q is the parameter in the neural network.

To handle the continuous space of control action, the policy gradient algorithm embedded NN is used to calculate the loss function. Hence, actor critic method is presented to combine the Q-learning and policy gradient algorithms [32], the actor aims to generate action by interacting with the environment, and the critic is responsible for evaluating the action. Finally, DDPG is

proposed to absorb the advantages of deep Q-learning and AC. The policy gradient of the loss function (actor-network) is calculated as follow:

$$\nabla l(\theta^{\varrho}) = E[(r + \beta Q(s_{t+1}, a_{t+1} | \theta^{\varrho}) - Q(s_t, a_t | \theta^{\varrho})) \nabla Q(s_t, a_t | \theta^{\varrho})] \quad (22)$$

where ∇ indicates the gradient function. The critic network is approximated by the Bellman equation [32]:

$$\begin{aligned} \nabla_{\theta^{\pi}} L &\approx E[\nabla_{\theta^{\pi}} Q(s_{t+1}, a_{t+1} | \theta^{\varrho})] \\ &= E[\nabla_a Q(s_t, a_t | \theta^{\varrho}) \nabla_{\theta^{\pi}} \pi(s_t | \theta^{\pi})] \end{aligned} \quad (23)$$

To modify the DDPG algorithm in this work, the DP-based optimal control policy or the real-world collected strategy is imported to optimize the search space of control actions. To narrow the search space, the related computational efficiency and performance would be improved. The pseudo-code of the modified DDPG algorithm is displayed in Table II. In this DRL framework, the learning rate α is 0.001, discount factor β is 0.95, the number of episodes is 1000, memory capacity and batch size in the NN is 2000 and 64, and ε is equal to $1 * 0.001^t$ (t is the time step). To estimate the proposed human-like EMS, the DDPG, DP, and DQL are compared in the next section. The optimality, convergence, and adaptability are proven by different designed experiments.

IV. ANALYZATION OF SIMULATION RESULTS

This section discusses the control performance of the proposed modified DDPG-based EMS (Human-like EMS). First, the optimality of the presented EMS is assessed by comparing with DP on a standard driving cycle. Then, on a real-world driving cycle1, the human-like EMS is evaluated via analyzing the comparative results among DDPG, DP, and DQL. Finally, the learned human-like control policy is estimated on another real-world driving cycle2 to reveal its adaptability for different driving situations in real-world environments.

A. Optimality of Modified DDPG

In the modified DDPG algorithm, the original space of control actions is limited by the DP-based control strategy (a sequence of control actions). Thus the optimality of the related EMS is guaranteed theoretically. To demonstrate this perspective, the human-like EMS is compared with DP to estimate its optimality on a standard driving cycle. Fig. 4 depicts the chosen cycle UDDS and two SoC trajectories in these two methods. It can be discerned that these two SoC curves are very close, so the output power of the battery is nearly the same (from Eq. (8), SoC is affected by P_b).

To display the power distribution between ICE and battery, Fig. 5 shows their power variation on the studied standard driving cycle (UDDS cycle). Since the ICE power is defined as the control action is this work, it is evident that the human-like EMS is almost same as the DP-based one (not all the same in the black circle). As DP can acquire the global optimal control policy via an exhaustive search process, the optimality of modified DDPG-enabled EMS is deduced. Compared with the conventional DDPG algorithm, the proposed control frame-

work is able to obtain optimal control actions with an efficient learning process.

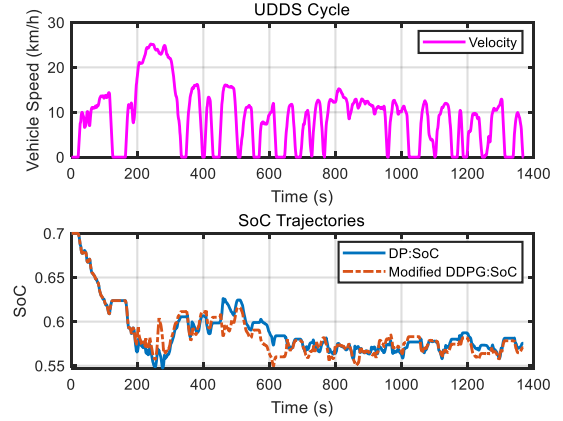


Fig. 4. SoC curves in DP and modified DDPG on the UDDS cycle.

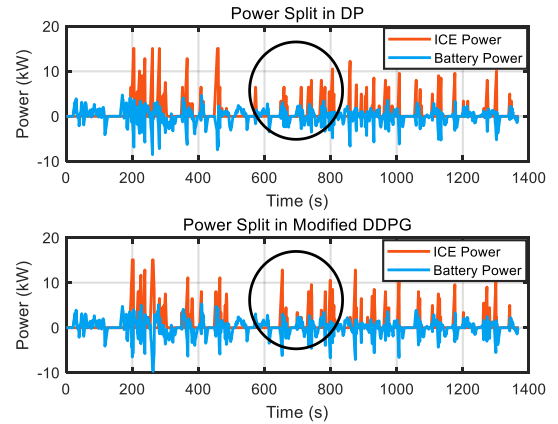


Fig. 5. Power distribution between ICE and battery in DP and modified DDPG.

B. Convergence Rate of Human-like EMS

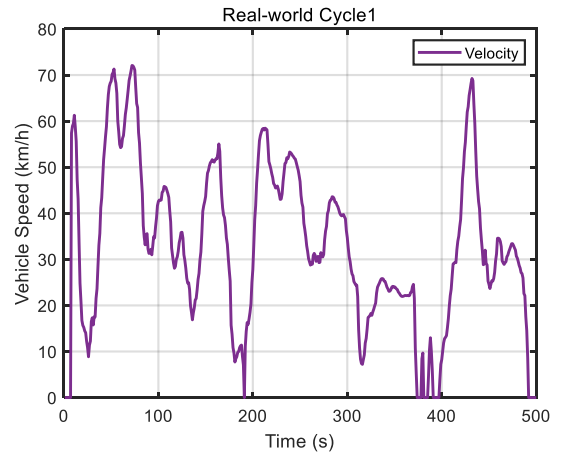


Fig. 6. Collected real-world cycle1 for human-like EMS generation.

In this subsection, a comprehensive analysis of four EMSs is conducted, and these policies are derived from modified DDPG, conventional DDPG, DQL, and DP. The setting parameters of DQL are the same as those in DDPG to ensure equitable comparison (three DRL methods). To generate human-like EMS for the series-parallel powertrain, a real-world driving cycle1 is leveraged in these four techniques, as described in Fig. 6. Furthermore, the SoC curves of these four situations are given in Fig. 7. In the modified DDPG approach, the search

space of control actions is composed of DP-based control policy and collected strategy from experienced human drivers. This design can ensure not only the optimality but also the human-like characteristics. As can be seen, the SoC trajectories in DQL and conventional DDPG are different from those in the other two cases, which indicates the control policies of these four cases are not identical. Thus, the convergence rate and control performance are further compared.

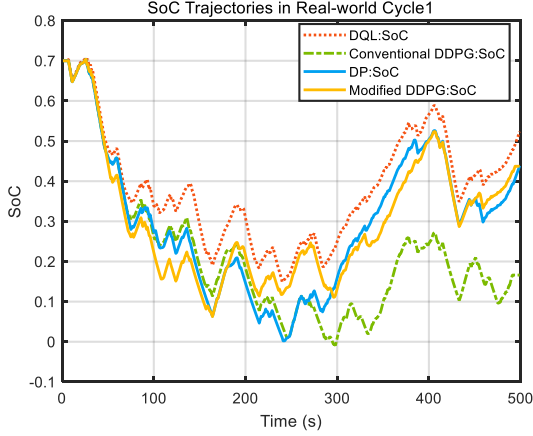


Fig. 7. SoC variations of four compared methods on real-world driving cycle1.

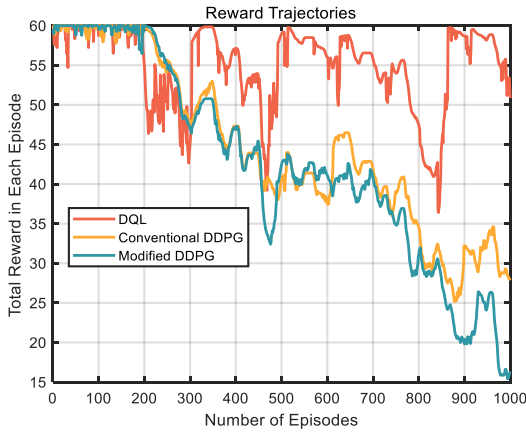


Fig. 8. A total reward of each episode in different DRL approaches.

TABLE III

EQUIVALENT FUEL CONSUMPTION FOR DIFFERENT DRL METHODS

Techniques [#]	Fuel Economy [*]	Training Time (hours)
DQL	108.9	10.72
Conventional DDPG	148.87	28.76
Modified DDPG	208.15	8.24

[#] A 2.90 GHz microprocessor with 7.83 GB RAM was used.

^{*} Equivalent fuel consumption, Unit: mpg (miles per gallon).

In Fig. 8, the total rewards in each episode of different DRL techniques are displayed (the number of training episodes is 1000). Since the reward represents the instantaneous cost function in Eq. (10), the proposed human-like EMS could achieve a better fuel economy with the same training episodes. It is caused by the diverse search spaces of control strategy in these situations. Hence, it can be concluded that the modified DDPG could promote the fuel economy. Table III shows the fuel consumption and training time of these three DRL-based EMSs. As the final value of SoC is not the same, the results in Table III are the equivalent fuel consumption, in which the

effects of differences of final SoC are disposed [33]. It is visualized that the modified DDPG (indicates the relevant human-like EMS) is capable of realizing the best control performance (indicates fuel economy and calculative efficiency). As the goal of human-like EMS is applied in real-world, the adaptability of this method is discussed in the next subsection.

C. Adaptability of Human-like EMS

To further explain the robustness of the built human-like control policy, three DRL-enabled control strategies are evaluated on another real-world driving cycle, as depicted in Fig. 9. In this experiment, the driving cycle in Fig. 9 is not included in the training process. It indicates the critic and actor networks are generated from real-world driving cycle1 (Fig. 6), and they will be applied on the driving cycle2 in Fig. 9. The simulation results could reveal that the EMS in Section IV.B would be adaptive to this new driving cycle or not. The relevant SoC trajectories in these three situations are also displayed in Fig. 9. The different variations of these SoC imply the obtained control actions are not the same, which indicates the output power and working points of ICE in these EMSs are different.

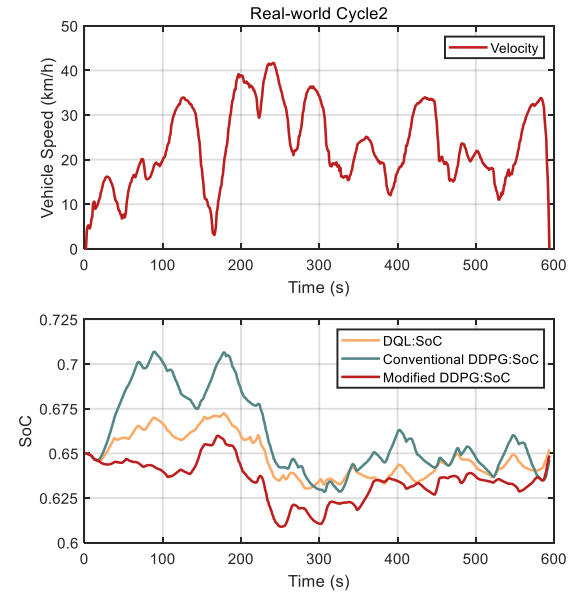


Fig. 9. SoC trajectories of different DRL approaches on a new driving cycle.

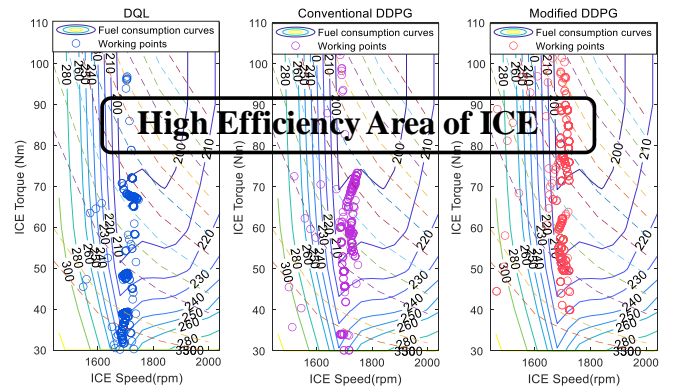


Fig. 10. Working points of ICE in different DRL methods on a new cycle.

Fig. 10 gives the working area of ICE in these three DRL approaches after the same training episodes. As the high-efficiency area is highlighted in this figure, the modified DDPG propels ICE to operate continually in this area. As a result, the ICE could consume less fuel to run the same driving

cycle. It can be ascribed to real-world driving experiences, which help the ICE and battery export power reasonably. Hence, the proposed human-like EMS could achieve better fuel economy than other methods, which demonstrates the adaptability of the presented control framework. Furthermore, this human-like EMS is possible to be applied in real-time by incorporating transfer learning thought, and it will be discussed in future work.

V. CONCLUSION

The purpose of this work is to speed up the training process of the conventional DDPG method. By considering the DP-based optimal control policy into the DRL framework, the optimality of the proposed EMS can be guaranteed. Furthermore, as we know, the experienced human drivers could manage power distribution according to the real-world driving conditions. Inspired by this motivation, the real-world driving dataset is collected, and a part of it is selected to construct the human-like control strategy. The collected power distribution between ICE and battery is taken as the expert knowledge to guide the choice of control in the DDPG algorithm. Owing to this operation, the intelligent agent could learn to run the hybrid powertrain as a human driver does. The designed experiments prove the optimality, convergence rate, and adaptability of the founded human-like EMS. Its control performance is better than the DQL and conventional DDPG, and further close to DP.

Future work could focus on combining the modified DDPG and transfer learning to formulate an online energy management system for hybrid vehicles. As the trained NN could be generalized to other real-world driving cycles, the relevant EMS has the potential to be applied in real-time environments. Moreover, the hardware-in-the-loop (HIL) experiment is able to be further constructed to demonstrate this research direction.

REFERENCES

- [1] T. Liu, X. Tang, H. Wang, H. Yu, and X. Hu, "Adaptive Hierarchical Energy Management Design for a Plug-in Hybrid Electric Vehicle," *IEEE Trans. Veh. Technol.*, vol. 68, no. 12, pp. 11513-11522, 2019.
- [2] Y. Huang, H. Wang, A. Khajepour, B. Li, J. Ji, K. Zhao, and C. Hu, "A review of power management strategies and component sizing methods for hybrid vehicles," *Renew Sustain Energy Rev.*, vol. 96, pp. 132-144, 2018.
- [3] T. Liu, X. Hu, W. Hu, Y. Zou, "A heuristic planning reinforcement learning-based energy management for power-split plug-in hybrid electric vehicles," *IEEE Trans. Ind. Informat.*, vol. 15, no. 12, pp. 6436-6445, 2019.
- [4] C. Martinez, X. Hu, D. Cao, E. Velenis, B. Gao, and M. Wellers, M. "Energy management in plug-in hybrid electric vehicles: Recent progress and a connected vehicles perspective," *IEEE Trans. Veh. Technol.*, vol. 66, no. 6, pp. 4534-4549, 2017.
- [5] T. Liu, H. Yu, H. Guo, Y. Qin, and Y. Zou, "Online energy management for multimode plug-in hybrid electric vehicles," *IEEE Trans. Ind. Informat.*, vol. 15, no. 7, pp. 4352-4361, July 2019.
- [6] W. Enang, and C. Bannister, "Modelling and control of hybrid electric vehicles (A comprehensive review)," *Renew Sustain Energy Rev.*, vol. 74, pp. 1210-1239, 2017.
- [7] X. Tang, D. Zhang, T. Liu, A. Khajepour, H. Yu, and H. Wang, "Research on the energy control of a dual-motor hybrid vehicle during engine start-stop process," *Energy*, vol. 166, pp. 1181-1193, 2019.
- [8] P. Zhang, F. Yan, and C. Du, "A comprehensive analysis of energy management strategies for hybrid electric vehicles based on bibliometrics," *Renew Sustain Energy Rev.*, vol. 48, pp. 88-104, 2015.
- [9] L. Li, C. Yang, Y. Zhang, L. Zhang, and J. Song, "Correctional DP-based energy management strategy of plug-in hybrid electric bus for city-bus route," *IEEE Trans. Veh. Technol.*, vol. 64, no. 7, pp. 2792-2803, 2015.
- [10] T. Liu, B. Wang, and C. Yang, "Online Markov Chain-based energy management for a hybrid tracked vehicle with speedy Q-learning," *Energy*, vol. 160, pp. 544-555, 2018.
- [11] H. Wang, Y. Huang, and A. Khajepour, "Cyber-Physical Control for Energy Management of Off-road Vehicles with Hybrid Energy Storage Systems," *IEEE/ASME Trans. Mechatronics*, vol. 23, no. 6, pp. 2609-2618, 2018.
- [12] T. Liu, and X. Hu, "A Bi-Level Control for Energy Efficiency Improvement of a Hybrid Tracked Vehicle," *IEEE Trans. Ind. Informat.*, vol. 14, no. 4, pp. 1616-1625, 2018.
- [13] M. Sabri, K. Danapalasingam, and M. Rahmat, "A review on hybrid electric vehicles architecture and energy management strategies," *Renew Sustain Energy Rev.*, vol. 53, pp. 1433-1442, 2016.
- [14] T. Liu, X. Hu, S. E. Li, and D. Cao, "Reinforcement learning optimized look-ahead energy management of a parallel hybrid electric vehicle," *IEEE/ASME Trans. Mechatronics*, vol. 22, no. 4, pp. 1497-1507, 2017.
- [15] X. Hu, T. Liu, X. Qi, and M. Barth, "Reinforcement Learning for Hybrid and Plug-In Hybrid Electric Vehicle Energy Management: Recent Advances and Prospects," *IEEE Trans. Ind. Electron. Magazine*, vol. 13, no. 3, pp. 16-25, 2019.
- [16] T. Liu, Y. Zou, D. Liu, and F. Sun, "Reinforcement learning of adaptive energy management with transition probability for a hybrid electric tracked vehicle," *IEEE Trans. Ind. Electron.*, vol. 62, no. 12, pp. 7837-7846, 2015.
- [17] Y. Zou, T. Liu, D. X. Liu, and F. C. Sun, "Reinforcement learning-based real-time energy management for a hybrid tracked vehicle," *Appl. Energy*, vol. 171, pp. 372-382, 2016.
- [18] J. Wu, H. He, J. Peng, Y. Li, and Z. Li, "Continuous reinforcement learning of energy management with deep Q network for a power split hybrid electric bus," *Applied energy*, vol. 222, pp. 799-811, 2018.
- [19] X. Qi, Y. Luo, G. Wu, K. Boriboonsomsin, and M. Barth, "Deep reinforcement learning enabled self-learning control for energy efficient driving," *Transportation Research Part C: Emerging Technologies*, vol. 99, pp. 67-81, 2019.
- [20] R. Lian, J. Peng, Y. Wu, H. Tan, and H. Zhang, "Rule-interposing deep reinforcement learning based energy management strategy for power-split hybrid electric vehicle," *Energy*, 117297, 2020.
- [21] Y. Wu, H. Tan, J. Peng, H. Zhang, and H. He, "Deep reinforcement learning of energy management with continuous control strategy and traffic information for a series-parallel plug-in hybrid electric bus," *Applied energy*, vol. 247, pp. 454-466, 2019.
- [22] S. Miller, "Hybrid Electric Vehicle Model in Simulink (<https://www.github.com/mathworks/Simscape-HEV-Series-Parallel>), GitHub. Retrieved June 19, 2020.
- [23] T. Liu, Y. Zou, and D. Liu, "Energy management for battery electric vehicle with automated mechanical transmission," *International Journal of Vehicle Design (IJVD)*, vol. 70, no. 1, pp. 98-112, 2016.
- [24] C. C. Lin, H. Peng, J. W. Grizzle, and J. M. Kang, "Power management strategy for a parallel hybrid electric truck," *IEEE Trans. Cont. Syst. Techn.*, vol. 11, no. 6, pp. 839-849, 2003.
- [25] Y. Zou, T. Liu, F. Sun, H. Peng, "Comparative study of dynamic programming and Pontryagin's minimum principle on energy management for a parallel hybrid electric vehicle," *Energies*, vol. 6, no. 4, pp. 2305-2318, 2013.
- [26] Z. Chen, C. C. Mi, J. Xu, X. Gong, and C. You, "Energy management for a power-split plug-in hybrid electric vehicle based on dynamic programming and neural networks," *IEEE Trans. Veh. Technol.*, vol. 63, no. 4, pp. 1567-1580, 2013.
- [27] J. Liu, J. Hagen, H. Peng, and Z. S. Filipi, "Engine-in-the-loop study of the stochastic dynamic programming optimal control design for a hybrid electric HMMWV," *International Journal of Heavy Vehicle Systems*, vol. 15, no. 2-4, pp. 309-326, 2008.
- [28] Qingkai Yang, "Study of the driving cycle of electric vehicles in Beijing," *Master Dissertation, Beijing Institute of Technology*, Jun. 2017. (in Chinese)
- [29] R. S. Sutton, A. G. Barto, Reinforcement learning: An introduction, *MIT press*, 2018.
- [30] Y. Liu, S. M. Cheng, and Y. L. Hsueh, "eNB selection for machine type communications using reinforcement learning based Markov decision process," *IEEE Trans. Veh. Technol.*, vol. 66, no. 12, pp. 11330-11338, 2017.
- [31] D. Silver, G. Lever, N. Heess, T. Degris, D. Wierstra, and M. Riedmiller, "Deterministic policy gradient algorithms," *In ICML*, June 2014
- [32] T. P. Lillicrap, J. J. Hunt, A. Pritzel, N. Heess, T. Erez, Y. Tassa, and D. Wierstra, "Continuous control with deep reinforcement learning," *arXiv preprint arXiv:1509.02971*, 2015.
- [33] C. Musardo, G. Rizzoni, Y. Guezennec, and B. Staccia, "A-ECMS: An adaptive algorithm for hybrid electric vehicle energy management. European Journal of Control, vol. 11, no. 4-5, pp. 509-524, 2013.